A Design of Experiment Analysis of Log-Normal Microsphere Distributions Modeling Drug Delivery

by

Jacob Nickle

A Thesis Presented in Partial Fulfillment
of the Requirements for the Degree
Master of Science

Approved July 2021 by the
Graduate Supervisory Committee:

Brent Vernon, Chair
Ryan McLemore
Scott Beeman

ARIZONA STATE UNIVERSITY

August 2021

ABSTRACT

Technology transfer hurdles constantly keep effective medical treatment from healthcare. One prevalent hurdle is that of cost. Regulation from any organization or entity can drive up cost and requires thorough review before implementation. For microspheres specifically, extensive research has been conducted to minimize variation in size. How variation effects drug delivery of microspheres, however, has not been studied in depth. In this study, a preliminary approach to modeling drug delivery in microspheres with a given log-normal distribution is reported. A design of experiment statistical analysis was performed using incremental values of mean and standard deviation. To estimate the rate of drug diffusing from the microspheres, a simplified Fick's second law was used. Various data types were considered and it was found that the shape factors which are related to mean and standard deviation fit the statistical analysis best. Using the shape factor data type, equation characteristics were identified and reported. It was seen that standard deviation has a greater influence on drug delivery than mean. A prediction expression is presented that can be used to identify the time it takes to get to 60% drug delivery and can be used in a scaled manner.

TABLE OF CONTENTS

Page

INTRODUCTION

Technology transfer has been a constant concern to many. One obvious and frequent obstacle to a successful transfer is that of cost [1]. When a novel technology is introduced, perceived improvement sometimes lead to more stringent regulation and cost. This causes a wider gap within technology transfer. One such technology is that of microspheres used as vehicles for sustained drug release. Since the first Food and Drug Administration(FDA) approval of clinical trials for naltrexone loaded polymeric spheres in 1984 [2], extensive improvements have been implemented on manufacturing including narrowing size distribution [3, 4, 5, 6, 7, 8]. Recently, the FDA has advised a control on variability [9]. This increase in regulation and technology leads to increased cost. Whether or not a larger size distribution results in a drug delivery that is well within satisfactory performance is not known and could depend largely on the distribution shape.

Modeling drug delivery from microspheres is a useful step to preliminary studies. Three prevalent diffusion drivers have been established depending on many characteristics such as the rate of degradation, drug loading, porosity and others [10]. In this study, it is assumed that the drug is uniformly distributed within each microsphere with diffusion being the primary method of drug delivery. Fick's second law in one dimension and with the product rule applied is as follows:

$$\frac{\partial C}{\partial t} = D(\frac{\partial^2 C}{\partial r^2} + \frac{2}{r}\frac{\partial C}{\partial r}) \tag{1}$$

Where C is the concentration, r is the radius, t is time and D is the diffusion coefficient. To further characterize the drug release, a semi-empherical equation can be used as developed by Korsmeyer et al. [11, 12] and is as follows:

$$\frac{M_t}{M_\infty} = kt^n \tag{2}$$

Where M_t is the cumulative amount of drug release, M_∞ is the cumulative drug released at infinite time, n is a diffusional exponent and k is a constant. An alternative form of equation 2 which can fit the cumulative release to a linear equation is shown as:

$$\log(\frac{M_t}{M_\infty}) = n\log(t) + \log(k) \tag{3}$$

The shape of the probability density function(PDF) representing a batch of microspheres depends on the method of fabrication. An in-depth discussion of which PDF best fits emulsion fabrication methods is discussed by Schuster et al. [13] and is suggested that a log-normal PDF is sufficient for many cases. If additional control is needed, there are other distributions that have been used and can be looked into for future research. For this study it is hypothesized that an equation can be formed such that drug delivery can be adequately predicted theoretically.

MATERIALS AND METHOD

Modeling

For mathematical modeling, the CAD software used was Wolfram Mathematica 11.3. In order to normalize equation 1, conditions were applied as shown in table 0.1. In this table, c_o, t_o, D_o and r_o are characteristic scaling constants.

$$C^* = \frac{c}{c_o} \;\Big|\; t^* = \frac{t}{t_o} \;\Big|\; D^* = \frac{D}{D_o} \;\Big|\; r^* = \frac{r}{r_o} \;\Big|\; t_o = \frac{r_o^2}{D}$$

Table 0.1: Shows conditions applied to normalize Fick's second law

$$c^*(1,t^*)=0 \mid c^*(r^*,0)=1 \mid \frac{\partial c^*}{\partial t^*}=c^*(r^*,t^*) \mid D=1 \mid c_o=1$$

Table 0.2: Shows boundary conditions and assumptions made to obtain a numeric result

Furthermore, boundary conditions and assumptions were applied as shown in table 0.2. The applied conditions and assumptions results in a solution to the simplified non-dimensional equation:

$$\frac{\partial C^*}{\partial t^*}=\frac{\partial^2 C^*}{\partial r^{*2}}+\frac{2}{r^*}\frac{\partial C*}{\partial r^*} \tag{4}$$

Once the solution($sol(r^*,t^*)$) was obtained from equation 4, it was then transferred into mass of drug released from each microsphere through time using the following equations:

$$\varpi_1(r_o,t^*)=4\pi r_o^3 c_o\int_0^1 sol(r^*,t^*)dr^* \tag{5}$$

$$\varpi_2(r_o,t)=\begin{cases}\varpi_1(r_o,\frac{t}{ro^2/D_o^*}) & \text{If } \frac{\partial C^*}{t^*}<0\\ 0 & \text{otherwise}\end{cases} \tag{6}$$

Equation 5 and equation 6 allowed differentiation of mass released between microsphere size. Furthermore D_o^* was assumed to be 1.

Within Mathematica, a mesh was created with automated range identified of both size of microsphere and time to optimise accuracy and reduce bias. Once the range was identified, a mesh was created with 1000 points, 100 levels for size and time. This mesh was then applied to equation 6. Afterwards, a trapezoidal integration was applied for the

r_o variable such that mass of drug delivery and time remain. Total initial mass of drug in all microspheres or $M\infty$ was then taken and used to calculate $\frac{M_t}{M\infty}$.

After the cumulative release curve was obtained($\frac{M_t}{M\infty}$), the data below 60% and then again above 20% of drug release was taken. The ranged data was then normalized according to mass of drug release at 60%. Furthermore, a log of base 10 was applied to the data after which a linear fit was applied. The slope and intercept was then extracted from the linear fit according to equation 3 and reported as the k and n characteristic constant response values.

Factors and Responses

Three different design of experiment factor types were considered. First, shape factors that form the PDF, second, mean(μ) and standard deviation(σ), and third, mean and fractional standard deviation(σ^o) where σ^o = (standard deviation / mean). This was done to potentially identify a superior data type for the design of experiment analysis.

To find quantitative values for the factors that will form the range for the design of experiment, relevant distribution values were pulled from three papers [14, 15, 16]. Using the data from the papers, the data types were then calculated. For transfer between shape factors and mean and standard deviation, the following equations were used:

$$mean = e^{\mu + \frac{\sigma^2}{2}} \tag{7}$$

$$stdev = \sqrt{(e^2 - 1)(e^{2\mu + \sigma^2})} \tag{8}$$

Where stdev is standard deviation, μ and σ are shape factors. Then max and min values were taken from each data type and used as the range for this study. Furthermore, it was decided to have four, equally spaced levels for each factor creating sixteen response values.

Response types are the k and n values from equation 2. The R^2 linear fit was also reported. In addition, the time value at 60% was also reported as an observation.

RESULTS

The actual by predicted plot of each data type for time to 60% drug release response can be seen in figure 0.1. Here it is seen that using a log base 10 transformation of the time to 60% drug release fits the prediction expression much better in each data type. For the shape factor data specifically, the R^2 value goes from 0.67 to 0.988 with the shape factor log transformation being the highest R^2 value. Furthermore, a contour plot for time to 60% drug release response is shown in figure 0.2 where a smooth consistent pattern is shown. It was decided to proceed with shape factor being the superior data type.

A further observation from the time to 60% drug release sub-figure 0.2a shows which shape factor has the greatest influence. The contour lines are less than 45° from horizontal, suggesting that the shape factor σ has a greater impact on the response than μ does. Quantities for each response are shown in table 0.3.

A linear fit for shape factors are shown in figures 0.4 and 0.5. It is seen in these figures that a linear fit of the data was achieved with an R^2 value not below 0.99 in any of the cumulative release plots. This validates the use of the characteristic constants(μ, σ), however, Korsmeyer's equation is being used for a distribution of microspheres instead of a single or monodisperse population.

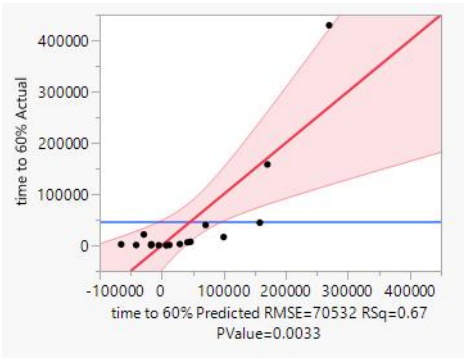

(a) Shape Factors

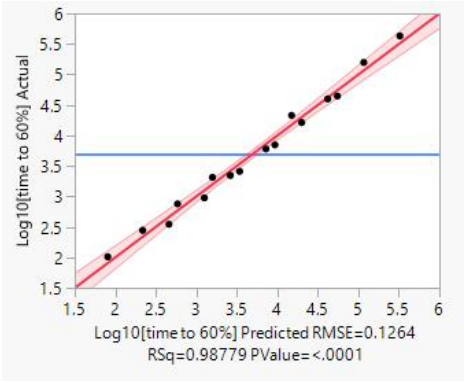

(b) Shape Factors

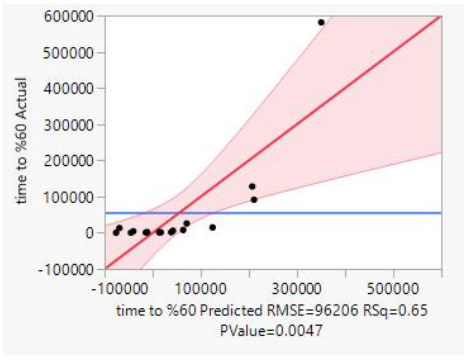

(c) mean and standard deviation

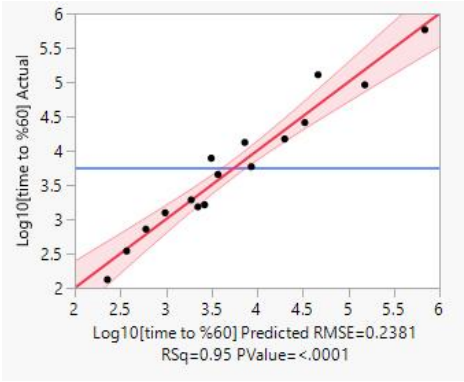

(d) mean and standard deviation d

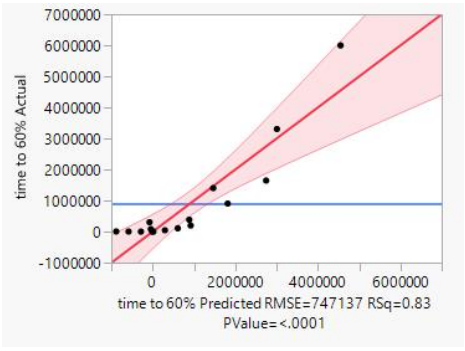

(e) mean and % standard deviation

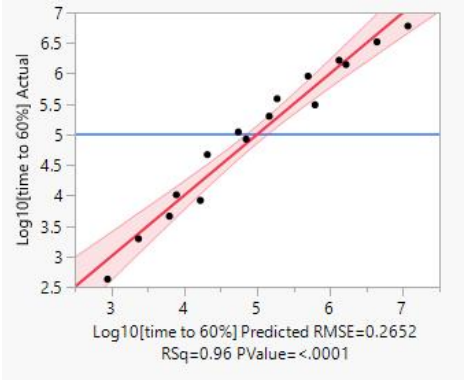

(f) mean and % standard deviation

Figure 0.1: Shows actual by predicted of each data type. Figures on left is for time to 60% drug release whereas figures on the right are for log base 10 of time to 60% drug release

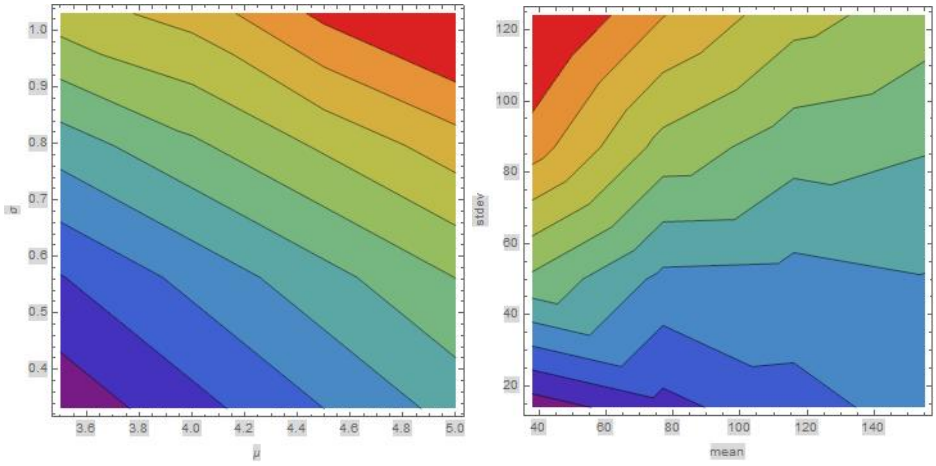

(a) shape factors: μ, σ (b) mean and standard deviation

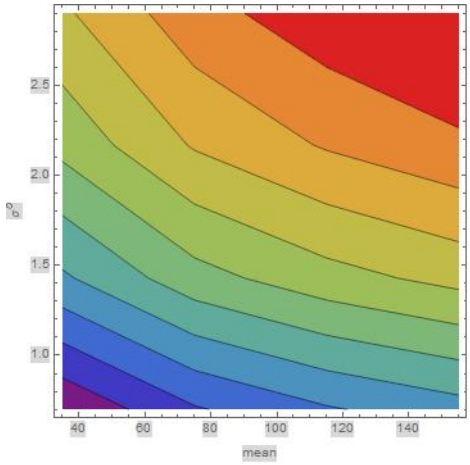

(c) mean and σ^o

Figure 0.2: Shows contour plots for log base 10 of time to 60% drug release for different data types. The red indicates a high response while the purple is low

Contour plots of the characteristic constants are shown in figure 0.3. In sub-figure 0.3a nearly throughout the entire response, it is clear that shape factor μ did not have an effect on the slope characteristic constant n with one exception. Furthermore, the intercept characteristic constant, k shows that both shape factors have close to equal impact with some exceptions.

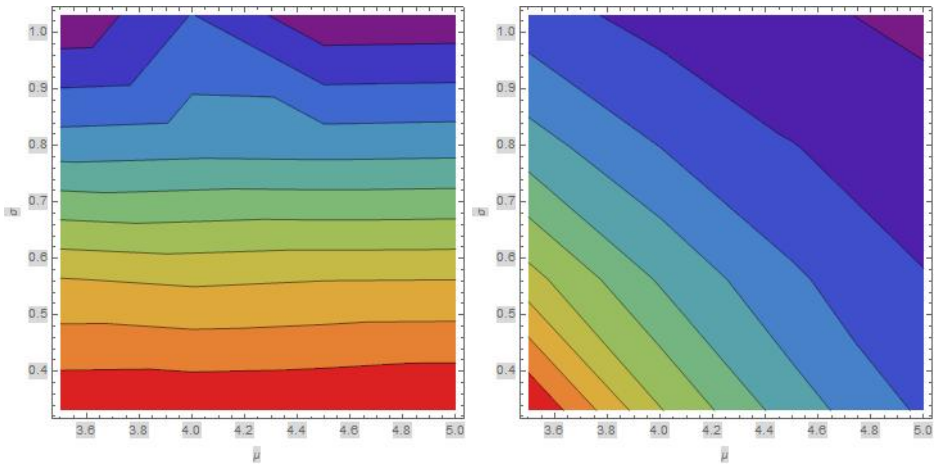

(a) n (b) k

Figure 0.3: Shows response contour plot of both characteristic constants k and n horizontal axes corresponds to the μ shape factor while the vertical axes is the σ shape factor as shown. Red color indicates maximum response while purple is minimum.

DISCUSSION

For this study it has been shown that a statistical equation can predict a drug release curve of a batch of microspheres without calculating each microsphere as long as the shape factors are known. This study was limited in that no variance was added for the design of experiments statistical analysis. Random variance could be artificially added and would be useful to see how it would effect the rate. Despite this, the prediction expression shown in table 0.6 gives a useful preliminary and theoretical way to predict drug delivery of a batch of microspheres instead of calculating each microsphere individually.

Another limitation in this study is the theoretical component. Some characteristics to microsphere drug delivery could deviate and effect the result including an initial burst release [17], diffusion mechanism [10] or other effects. For this reason, a future in vitro benchtop study is needed before recommendations to manufacturing and regulations are made.

Although it has limitations, this study is useful because it attempts to understand the effect of polydispersity on drug delivery of microspheres which the FDA acknowledges has an effect but does not explain how [18]. Here we have shown that shape factor μ does not have an effect on the slope characteristic constant n while it does for k defined by Korsmeyer et al. [11, 12]. This shows that the shape of drug delivery through time depends on variance. A brief consideration on a linear cumulative curve shows a n value not above 0.05. This suggests that as the shape factor σ quantity grows, it approaches a linear equation.

It should be noted, however, that one response value from the shape factor n did not have an expected result as shown in the sub-figure 0.3a. There are may reasons why this could occur including frequency sampling, rounding error, estimations, numeric computation and so forth. Future studies should identify this unexpected result.

As future studies of understanding the specific effects of variation have on microspheres continue, further calculated development of this technology can reach more patients in need of specialised drug delivery vehicles. This can be done by easing restrictions on manufacturing processes of microspheres without jeopardizing its safety or effect. In this study, this area of research has been highlighted and will hopefully inspire others to investigate as well.

BIBLIOGRAPHY

[1] V. Choudhry, T. A. Ponzio, Modernizing federal technology transfer metrics, The Journal of Technology Transfer 45 (2) (2020) 544–559.

[2] N. Goonoo, A. Bhaw-Luximon, R. Ujoodha, A. Jhugroo, G. K. Hulse, D. Jhurry, Naltrexone: a review of existing sustained drug delivery systems and emerging nano-based systems., Journal of Controlled Release 183 (1) (2014) 154–166.

[3] P. Sansdrap, A.-J. Moës, Influence of manufacturing parameters on the size characteristics and the release profiles of nifedipine from poly (dl-lactide-co-glycolide) microspheres, International journal of pharmaceutics 98 (1-3) (1993) 157–164.

[4] B. Amsden, M. Goosen, An examination of factors affecting the size, distribution and release characteristics of polymer microbeads made using electrostatics, Journal of controlled release 43 (2-3) (1997) 183–196.

[5] K. Shiga, N. Muramatsu, T. Kondo, Preparation of poly (d, l-lactide) and copoly (lactide-glycolide) microspheres of uniform size, Journal of pharmacy and pharmacology 48 (9) (1996) 891–895.

[6] B. Amsden, The production of uniformly sized polymer microspheres, Pharmaceutical research 16 (7) (1999) 1140.

[7] N. Leelarasamee, S. Howard, C. Malanga, J. Ma, A method for the preparation of polylactic acid microcapsules of controlled particle size and drug loading, Journal of microencapsulation 5 (2) (1988) 147–157.

[8] C. Berkland, K. K. Kim, D. W. Pack, Fabrication of plg microspheres with precisely controlled and monodisperse size distributions, Journal of controlled release 73 (1) (2001) 59–74.

[9] Food and Drug Administration, et al., Drug products, including biological products, that contain nanomaterials-guidance for industry (2018).

[10] D. Y. Arifin, L. Y. Lee, C.-H. Wang, Mathematical modeling and simulation of drug release from microspheres: Implications to drug delivery systems, Advanced Drug Delivery Reviews 58 (12) (2006) 1274–1325.

[11] R. W. Korsmeyer, S. R. Lustig, N. A. Peppas, Solute and penetrant diffusion in swellable polymers. i. mathematical modeling, Journal of Polymer Science Part B 24 (2) (1986) 395–408.

[12] R. W. Korsmeyer, E. V. Meerwall, N. A. Peppas, Solute and penetrant diffusion in swellable polymers. ii. verification of theoretical models, Journal of Polymer Science Part B 24 (2) (1986) 409–434.

[13] D. Schuster, Encyclopedia of emulsion technology: basic theory, Vol. 1, CRC Press, 1983.

[14] Y. Bahl, H. Sah, Dynamic changes in size distribution of emulsion droplets during ethyl acetate-based microencapsulation process, Aaps Pharmscitech 1 (1) (2000) 41–49.

[15] B. P. D. Smet, D. Poncelet, R. Neufeld, Control of mean diameter and size distribution during formulation of microcapsules with cellulose nitrate membranes, Enzyme and Microbial Technology 11 (1) (1989) 29–37.

[16] B. P. D. Smet, R. J. Neufeld, D. Poncelet, Preparation of hemolysate-filled hexamethylene sebacamide microcapsules with controlled diameter, Canadian Journal of Chemical Engineering 68 (3) (1990) 443–448.

[17] X. Huang, C. S. Brazel, On the importance and mechanisms of burst release in matrix-controlled drug delivery systems, Journal of controlled release 73 (2-3) (2001) 121–136.

[18] M. Martinez, M. Rathbone, D. Burgess, M. Huynh, In vitro and in vivo considerations associated with parenteral sustained release products: a review based upon information presented and points expressed at the 2007 controlled release society annual meeting, Journal of Controlled Release 129 (2) (2008) 79–87.

APPENDIX A

TABLES OF RESULTS

Pattern	μ	σ	n	k [11, 12]	Time to 60%
11	3.5	0.33	0.449996	0.0765	102.485
12	3.5	0.5633	0.42668	0.0508381	349.958
13	3.5	0.7966	0.389655	0.0308284	2213.45
14	3.5	1.03	0.362078	0.0167537	21388.2
21	4	0.33	0.45029	0.048754	278.444
22	4	0.5633	0.424976	0.0335659	949.344
23	4	0.7966	0.390679	0.0207129	6015.02
24	4	1.03	0.377567	0.0113564	39799
31	4.5	0.33	0.450844	0.0309704	756.9
32	4.5	0.5633	0.426087	0.0217563	2581.78
33	4.5	0.7966	0.390253	0.0140824	16315
34	4.5	1.03	0.362817	0.00805629	157969
41	5	0.33	0.452311	0.019529	2057.55
42	5	0.5633	0.426296	0.141877	7017.51
43	5	0.7966	0.390782	0.0094799	44336.8
44	5	1.03	0.363195	0.00557887	429458

Table 0.3: Shows results of shape factor design of experiments

Pattern	mean	stdev	n	k [11, 12]	Time to 60%
11	38	14	0.448435	0.0688269	132.272
12	38	50	0.364807	0.023587	7781.96
13	38	87	0.354167	0.00960324	128015
14	38	124	0.362993	0.00500086	581312
21	77	14	0.459821	0.0418117	344.84
22	77	50	0.419883	0.0277001	1630.83
23	77	87	0.372799	0.0172604	14825.9
24	77	124	0.353674	0.0108819	91293.6
31	116	14	0.458417	0.0300446	718.759
32	116	50	0.447187	0.0233271	1519.19
33	116	87	0.410515	0.0176016	5855.97
34	116	124	0.377448	0.0134016	25744.4
41	155	14	0.460816	0.0229721	1245.7
42	155	50	0.452689	0.0200845	1918.67
43	155	87	0.432762	0.0162282	4503.94
44	155	124	0.402399	0.0135922	13226.1

Table 0.4: Shows results of Mean and standard deviation design of experiment results

Pattern	mean	stdev	n	k [11, 12]	Time to 60%
11	35	0.7	0.413434	0.0507253	423.7
12	35	1.43	0.358328	0.0226114	10251.6
13	35	2.17	0.352181	0.011395	83940.1
14	35	2.9	0.360051	0.00654752	306615
21	75	0.7	0.417129	0.0263078	1947.26
22	75	1.43	0.358981	0.013042	46732.2
23	75	2.17	0.353104	0.00658367	386071
24	75	2.9	0.358616	0.00385903	1404670
31	115	0.7	0.415132	0.0187194	4571.79
32	115	1.43	0.360972	0.00938748	109945
33	115	2.17	0.356479	0.0046603	906153
34	115	2.9	0.359274	0.00281185	3305500
41	155	0.7	0.415317	0.0145897	8299
42	155	1.43	0.360849	0.00758211	199364
43	155	2.17	0.35346	0.00392564	1647480
44	155	2.9	0.359667	0.00225645	6000340

Table 0.5: Shows results of mean and %Standard Deviation

Multiplier			$\frac{x-4.25}{0.75}$	$\frac{y-0.68}{0.35}$	$\frac{x-4.25}{0.75}\frac{y-0.68}{0.35}$
n	$\sum$	0.4084035285	-3.7061$\times 10^{-}5$	-0.043351269	-1.208282 $\times 10^{-}3$
Log_{10} [k]	$\sum$	-1.691422312	-0.266733785	-0.302058948	0.029920087
Log_{10} [time]	$\sum$	3.6983646986	0.6573285718	1.1454802309	0.0110518254

Table 0.6: Shows prediction expressions for shape factors as a result of a design of experiment analysis

Multiplier			$\frac{x-96.5}{58.5}$	$\frac{y-69}{55}$	$\frac{x-96.5}{58.5}\frac{y-69}{55}$
n	$\sum$	0.4109873493	0.027862029	-0.041448146	6.6448695 $\times 10^{-}3$
Log$_{10}$ [k]	$\sum$	-1.722852115	0.0095576761	-0.289022165	0.2217998641
Log$_{10}$ [time]	$\sum$	3.7634265156	-0.335115573	1.088921683	-0.652061963

Table 0.7: Shows prediction expressions for mean and standard deviation data type as a result of a design of experiment analysis

Multiplier			$\frac{x-95}{60}$	$\frac{y-1.8}{1.1}$	$\frac{x-95}{60}\frac{y-1.8}{1.1}$
n	$\sum$	0.372060875	7.4715 $\times 10^{-}4$	-0.025990105	-3.32422 $\times 10^{-}4$
Log$_{10}$ [k]	$\sum$	-2.048366389	-0.240061493	-0.421678428	0.0172004262
Log$_{10}$ [time]	$\sum$	5.0083176849	0.6367588957	1.4225754783	2.345596 $\times 10^{-}4$

Table 0.8: Shows prediction expressions for mean and percent standard deviation data type as a result of a design of experiment analysis

APPENDIX B

FIGURES OF RESULTS

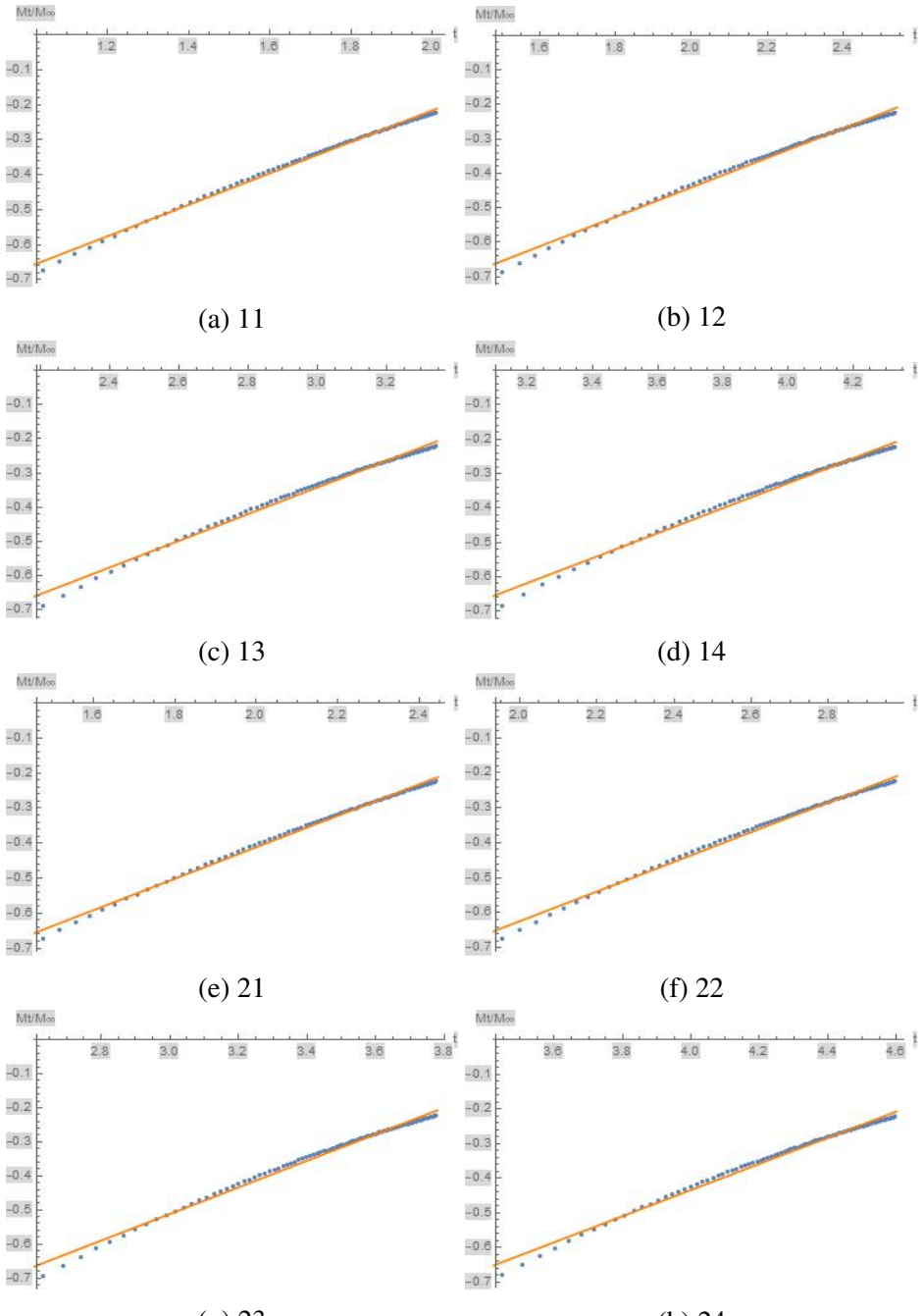

(a) 11 (b) 12

(c) 13 (d) 14

(e) 21 (f) 22

(g) 23 (h) 24

Figure 0.4: Shows linear fit of data for observations 11 to 24 for the shape factor design of experiment. X axes is time and Y axes is normalized mass of drug. Orange line is the linear fit while the blue dots are the meshed data.

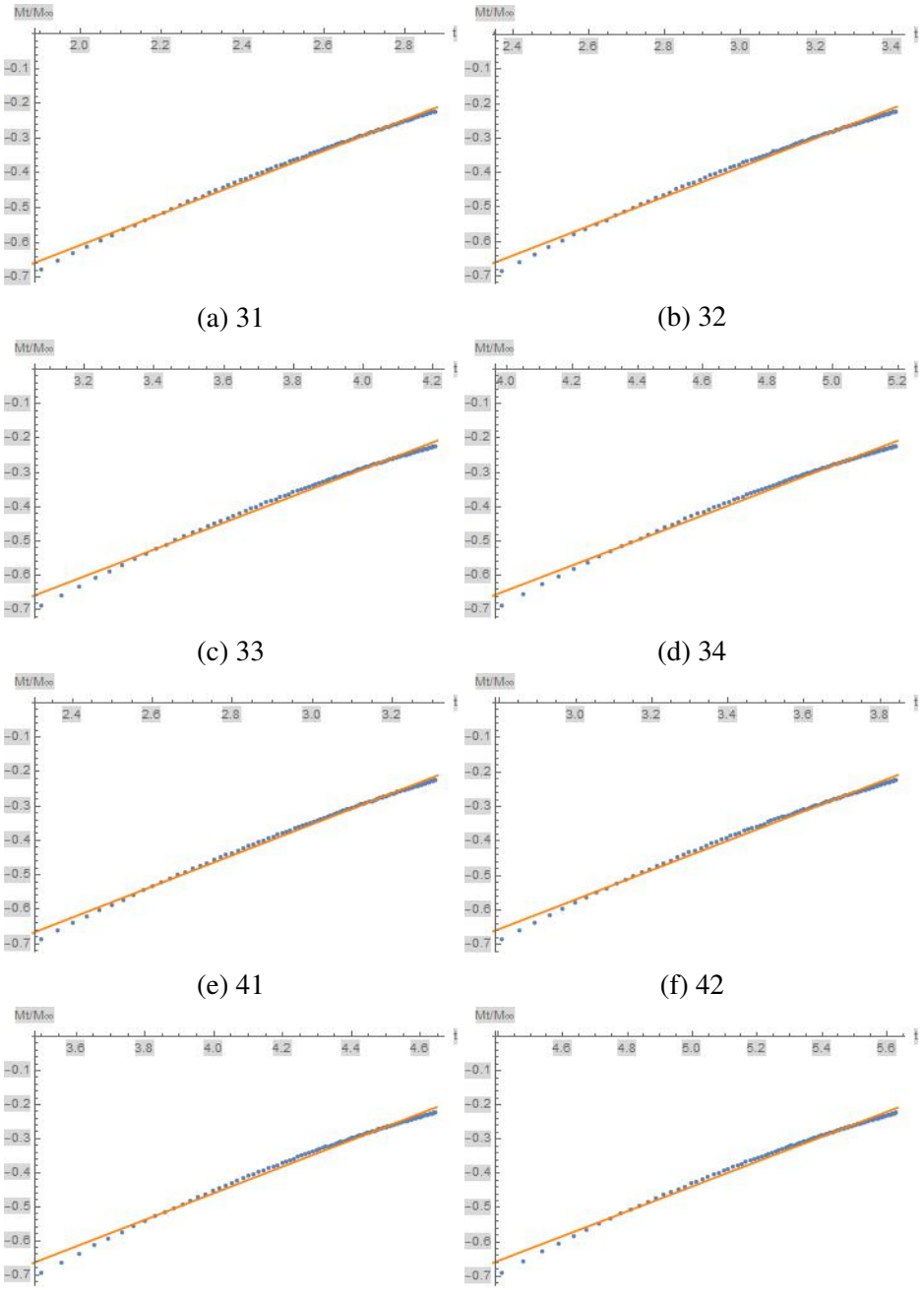

(a) 31 (b) 32

(c) 33 (d) 34

(e) 41 (f) 42

(g) 43 (h) 44

Figure 0.5: Shows linear fit of data for observations 31 to 44 for the shape factor design of experiment. X axes is time and Y axes is normalized mass of drug. Orange line is the linear fit while the blue dots are the meshed data.

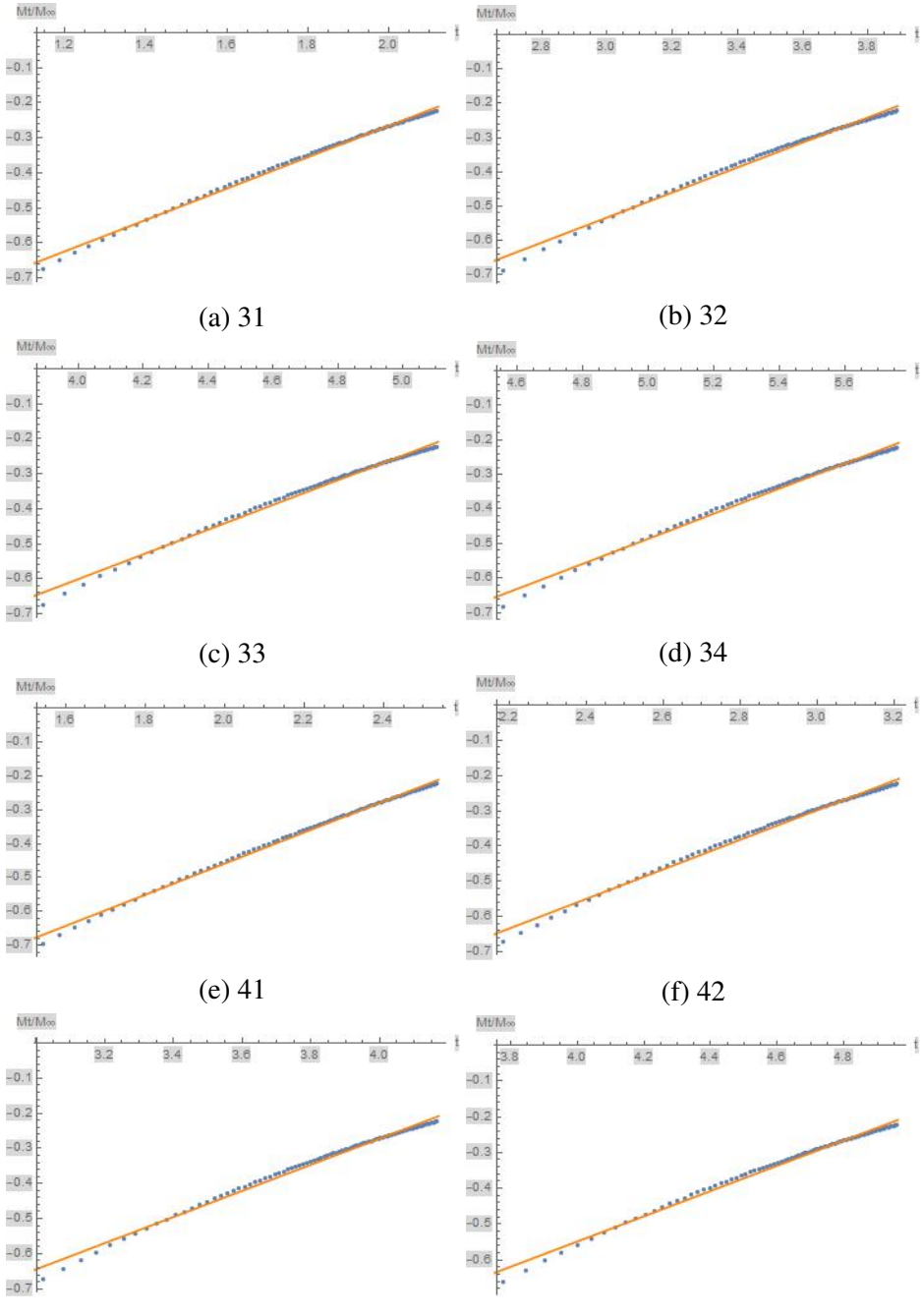

Figure 0.6: Shows linear fit of data for observations 11 to 24 for the Mean and Standard deviation design of experiment. X axes is time and Y axes is normalized mass of drug. Orange line is the linear fit while the blue dots are the meshed data.

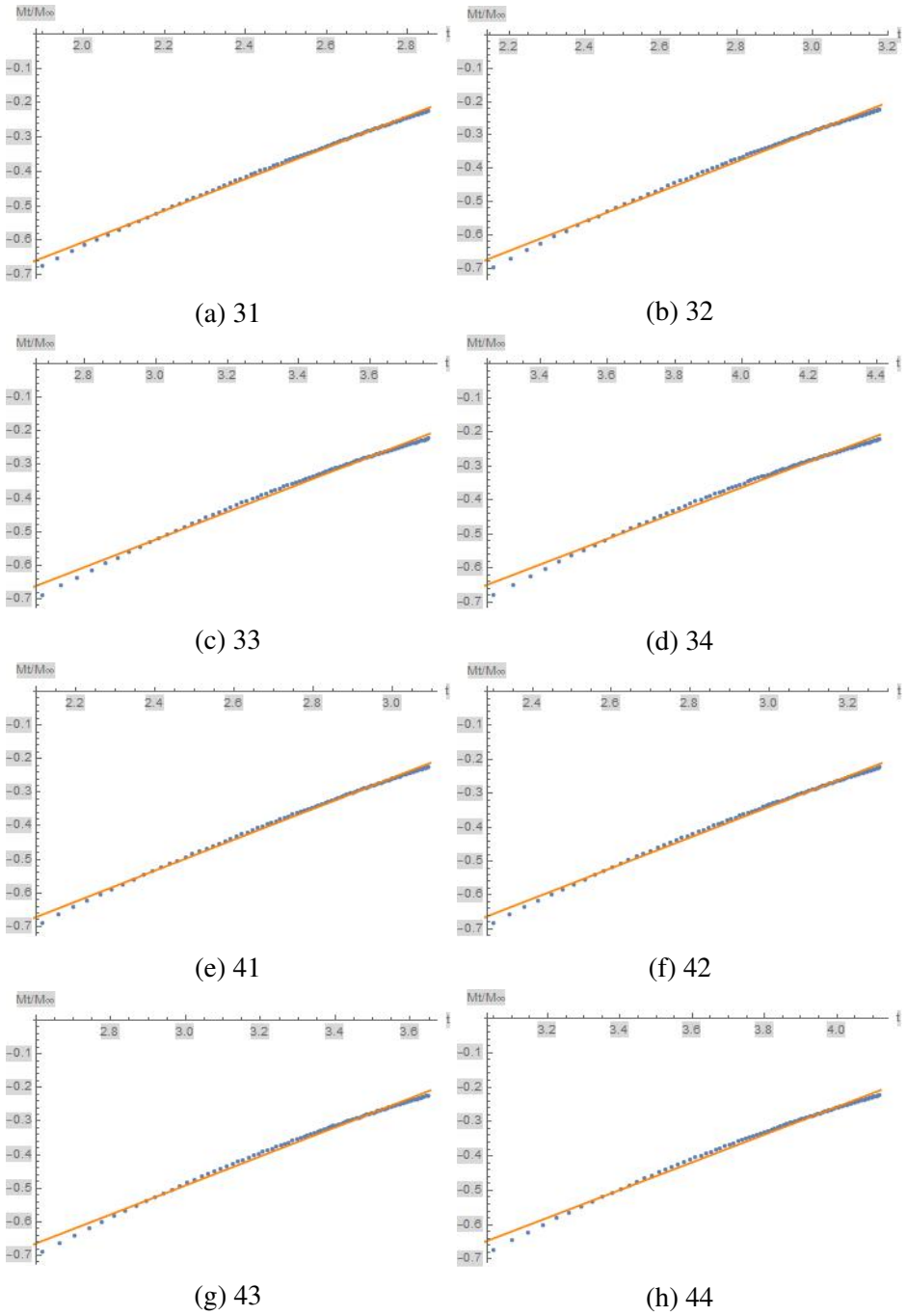

Figure 0.7: Shows linear fit of data for observations 31 to 44 for the Mean and Standard deviation design of experiment. X axes is time and Y axes is normalized mass of drug. Orange line is the linear fit while the blue dots are the meshed data.

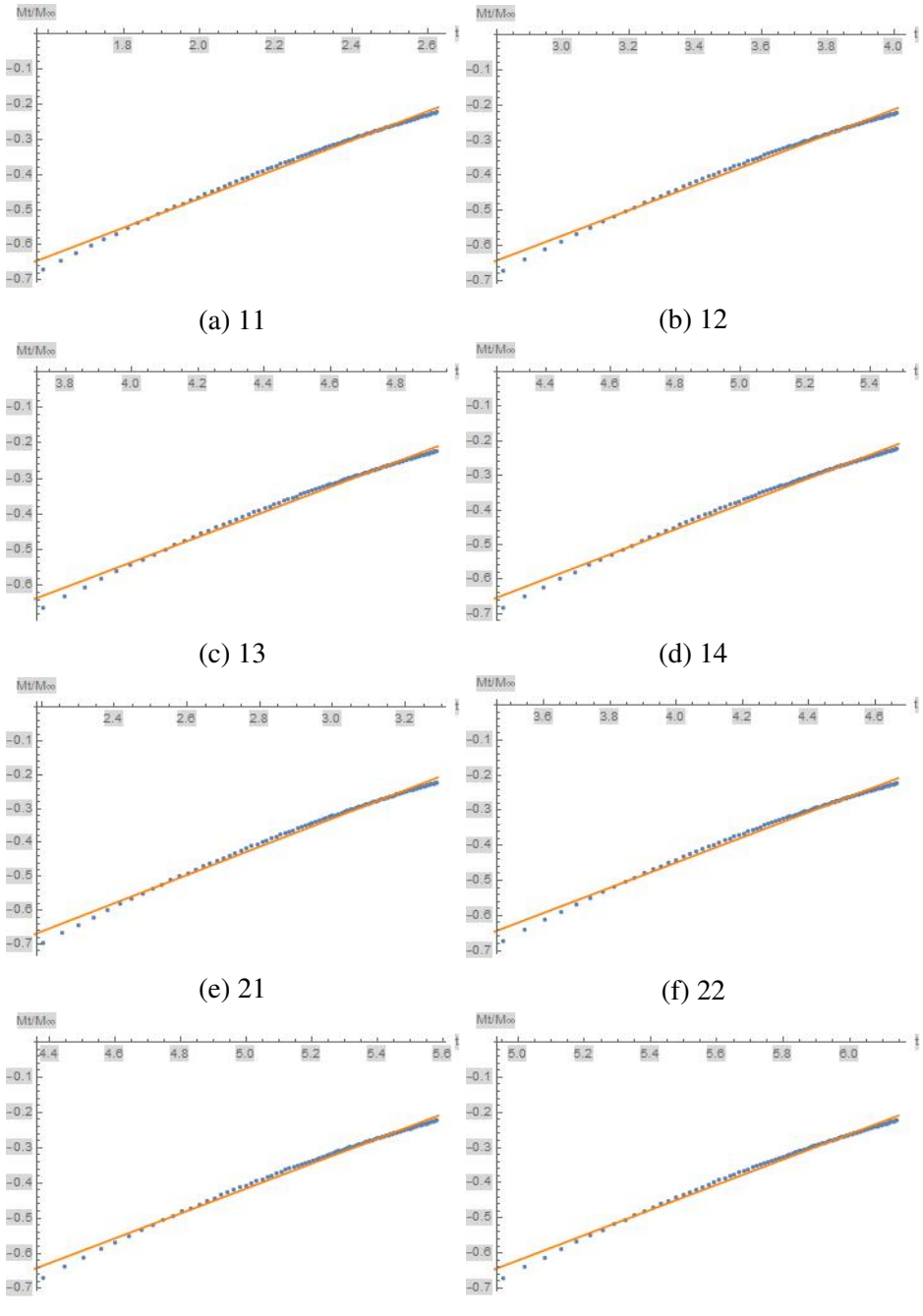

Figure 0.8: Shows linear fit of data for observations 11 to 24. X axes is time and Y axes is normalized mass of drug. Orange line is the linear fit while the blue dots are the meshed data.

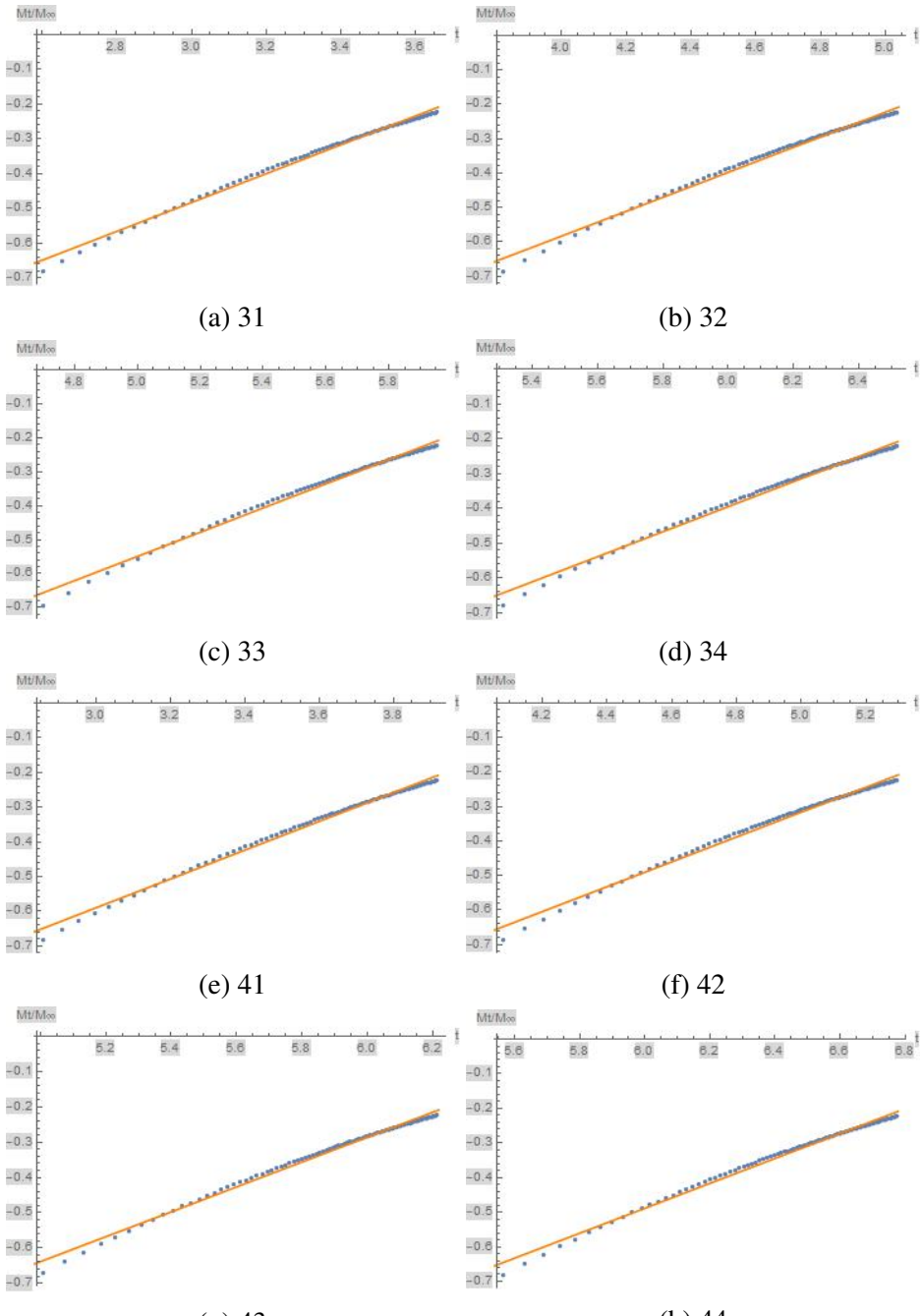

(a) 31 (b) 32

(c) 33 (d) 34

(e) 41 (f) 42

(g) 43 (h) 44

Figure 0.9: Shows linear fit of data for observations 31 to 44. X axes is time and Y axes is normalized mass of drug. Orange line is the linear fit while the blue dots are the meshed data.